

Article

A Feasibility Analysis of Controlling a Hybrid Power System over Short Time Intervals

Tianyao Zhang ¹, Diyi Chen ^{1,2,*}, Jing Liu ¹, Beibei Xu ¹ and Venkateshkumar M ³ 

¹ Institute of Water Resources and Hydropower Research, Northwest A&F University, Yangling 712100, China; zzttyy@nwfau.edu.cn (T.Z.); ljliujing1995@163.com (J.L.); beibeixu@nwsuaf.edu.cn (B.X.)

² Key Laboratory of Agricultural Soil and Water Engineering in Arid and Semiarid Areas, Ministry of Education, Northwest A&F University, Yangling 712100, China

³ Department of Electrical and Electronics Engineering, Amrita School of Engineering, Amrita Vishwa Vidyapeetham, Chennai 601103, India; m_venkateshkumar@ch.amrita.edu

* Correspondence: diyichen@nwsuaf.edu.cn

Received: 25 September 2020; Accepted: 27 October 2020; Published: 30 October 2020



Abstract: Literature about the importance of renewable energy resources, including wind and solar energy, is becoming increasingly important; however, these energy sources are unstable and volatile in nature, and are usually integrated with conventional energy sources, such as hydropower, forming hybrid power generation systems that maintain a stable grid. Short-term changes in wind speed or solar radiation intensity have a great impact on the stability of hybrid systems, and have been reported in the literature. However, reliable models to manage such systems are lacking, and previous studies have regarded the hour scale as the minimum baseline for systematic change. In this article, hybrid power systems are proposed that are controlled on very short time intervals. The results of a feasibility analysis of the proposed model indicate the viability of complementary hybrid systems in controlling and maintaining the stability, which are subjected to short durations of fluctuations in wind or solar radiation. The simulation results indicate that the influence of the shutdown of the wind turbine, with the regulation effect of the hydro power, is 3–5 times greater than that of the short-term wind turbulence fluctuation. When the hydro turbine is adopted to adjust the short-term fluctuation of solar radiation, the effect on the system was suppressed to 0.02–0.2 times of the former.

Keywords: hybrid system; wind speed fluctuation; solar radiation fluctuation; short time interval; hydro regulation

1. Introduction

With the exploitation of fossil energy reaching its limits [1], many countries are paying great attention to renewable energy sources [2,3], such as solar [4], wind [5,6], hydro [7,8], and other [9,10] energy, for their environmentally friendly characteristics [11]. High proportions of renewable energy have become key to solving the issues of global warming and air pollution in many countries [12], especially in China [13]. However, wind power and photovoltaic power have randomness, fluctuations [14], and intermittence [15], which lead to the toggling of the stability of these power systems, and then causes fluctuations in the power supply of the grid [16]. Hydropower, as a large-scale power source with a good regulation performance [17], has the ability to suppress fluctuation generated in solar and wind power systems, thereby improving their power grid capacity [18,19]. The methods of regulating the fluctuations in the power output of wind and solar energy systems with hydropower have been widely studied [20], and the stability analysis of power output is therefore an important aspect of research on hybrid-energy complementary systems.

Current research indicates the feasibility of multi-energy source complementation, and also points out the effects of fluctuations in wind speed or solar radiation intensity on hybrid systems, which occur due to conditions, such as high wind speed and cloud cover. Duque et al. used assessment parameters from different case studies, by focusing on the economic, reliability, environmental, and social factors related to wind-hydro hybrid systems, to optimise the operation of such systems [21]. Li et al. proposed an optimization model using a long-term multi-objective algorithm for a hybrid solar and hydro-electric system, by considering the fluency and annual power output of the system [22]. Liu et al. established the sizing method of a hydro-PV-pumped storage integrated generation system, and analysed the economy and complementarity of the model [23]. In the above literature, when analyzing the regulation effect of a hydro turbine on solar or wind power, the fluctuation of wind speed and solar radiation is mild and slow, ignoring the short and sharp mutation that the intermittency renewable energies may cause. In the hydropower-dominant hybrid system, the hydro turbine response should be further analyzed under the short-term fluctuation of wind and solar energy, to avoid the possible short-time overload of the hybrid system.

For the analysis time scale, previous studies of the hydro power regulation effect on intermittency energies, which mainly adopted the hour scale as the minimum complementary time scale, with the scheduling, control, and management of power generation units have often been carried out through manual interventions. Dufo-Lopez et al. described a novel methodology for optimal performance to control standalone systems with hybrid systems using hour-long time intervals [24]. Zhang et al. explored the wind-photovoltaics-hydro complementary clean energy system in the certain example, and used a progress optimality algorithm for the optimal operation of the system in day-long time intervals [25]. To suppress energy fluctuations, the manual-based scheduling plan is usually carried out on the time scale of hours or days; however, such methods are time-consuming and may cause the hybrid system to overload. Hence, the starting point of this paper was to enable the hybrid system to be adaptive and stable in the era of information and intelligence, by using the hydro turbine's adaptive regulation effect, replacing the manual scheduling, and thus enhancing the power grid's ability to include wind and solar energy sources. Combined with the questions in the preceding paragraph, a model with a minimum time scale of an hour cannot adequately describe the overload conditions that occur due to short-term fluctuations; hence, research with reduced time scales should be conducted to study the operational characteristics of hydro turbines, which are used to suppress fluctuations of energy and maintain the stability of multi energy systems over short time intervals [26,27].

In light of the above shortages, the novelty of this paper includes three aspects. First, to break the conventional scheduling method of hybrid power systems in an hour scale, this paper develops the study from an hour scale to a sub-hour scale. All of the analyses based on a relatively shorter calculated step will enable the results to become more self-adaptive in comparison to the conventional manual scheduling management. Second, aiming at a stability problem caused by the short-term mutation of wind speed and solar radiation, this paper proves the positive impact of the hydropower system in balancing the power fluctuation of these intermittency renewable energies. Simultaneously, the necessity of hydropower in regulating the short-term power fluctuation is also revealed. Third, based on four evaluation indices, the effect of hydropower on the power fluctuation is quantified under various scenarios. The obtained results will significantly contribute to improving the safety operation of hybrid power systems.

The research work is presented in a structured way as follows: the model and method adopted in this paper are presented in Section 2. The feasibility analysis of a complementary hybrid system under short-term fluctuation is detailed in Section 3. In Section 4, a simulation of the complementary output of the hybrid system is presented. Finally, the conclusions based on the results of the study are presented in Section 5.

2. Models and Methods

The proposed hybrid system simulated for this study consists of a wind turbine (WT), photovoltaic system (PV), hydraulic turbine (HT), and complementary platform. This hybrid system will be adopted as an example to simulate the system output power, and the modelling structure is presented in Figure 1. The research method adopts the short time scale evaluation indicators, which are used to analyze the hybrid system output under the short-term fluctuation of wind speed of solar radiation.

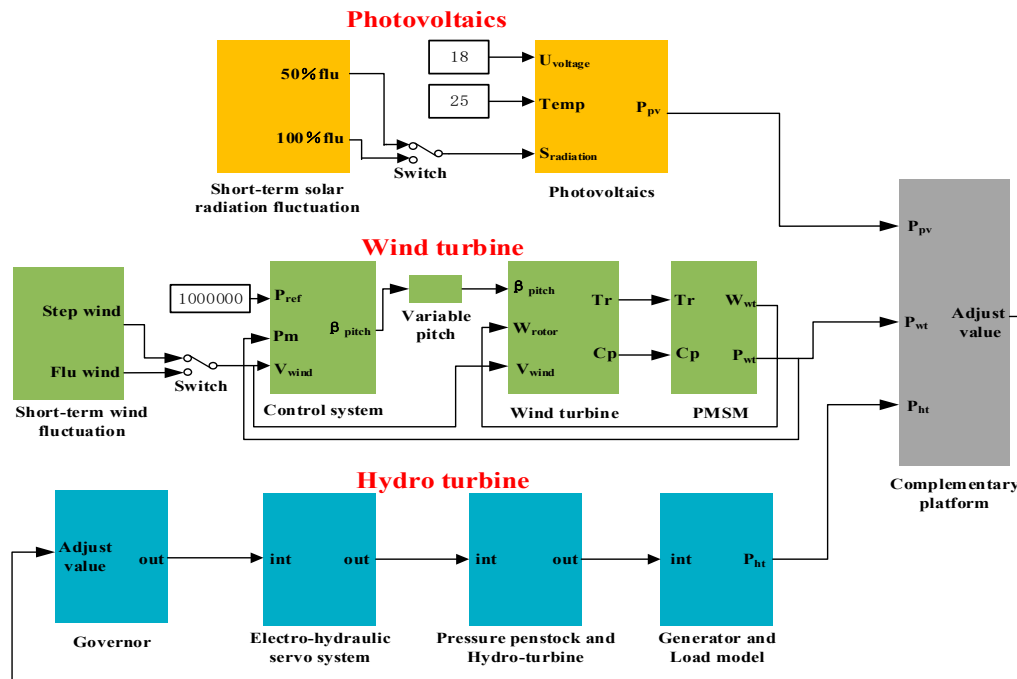


Figure 1. Hybrid system model.

2.1. Short Time Scale Analysis Method

The method of analyzing the output of the hybrid system under a short time scale is presented in Figure 2, and is fulfilled in four steps. The proposed method has been validated in a long-term scale but has not been tested on the short-term time scale.

- Step 1 Based on the long-term scale, several indicators are adopted for evaluating the output of the short-term scale system, namely t_s , R , W , and α .
- Step 2 The wind turbine (WT), photovoltaics (PV), and hydro turbine (HT) generation model were established respectively, enumerating and quantifying the various wind speed and photovoltaic short-time fluctuations J .
- Step 3 To attain the smooth output operational characteristics in the hybrid system, by referring to the solar and wind energy national standard of $t_{regulation}$ and $R_{regulation}$, and analyzing the output characteristics of WT and PV under various fluctuations J .
- Step 4 When certain wind speed fluctuation leads to the wind turbine output being beyond the standard, hydro turbine regulation will be adopted; then, the hybrid system output is simulated and evaluated. The same analysis method will be used to analyze the short-term fluctuations in solar power regulated by the hydro turbine.

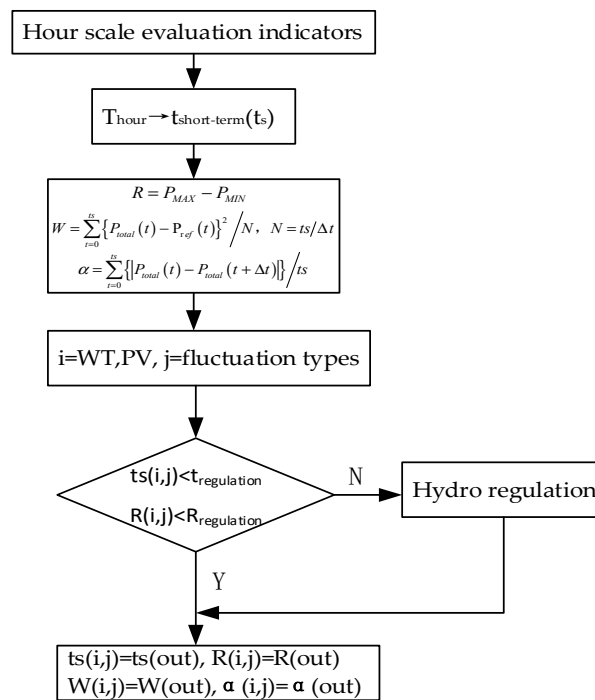


Figure 2. Flow chart of the simulation method.

2.2. Evaluation Indicators

In this paper, the active output power of a combined generation system is evaluated for four different indicators: fluctuation time, variation range, active power deviation, and the summation of peak and valley slopes.

- *Fluctuation time t_s*

When external disturbance of wind and solar energy occurs, the fluctuation time is used to describe the adjustment time required for the hybrid system to reach a stable state, and it is used as the time step to evaluate the other three indicators.

- *Variation range R*

The calculation method of R represents the system output range. An increase in R indicates an increase in the range of the system output variation:

$$R = P_{MAX} - P_{MIN}, \quad (1)$$

where P_{MAX} is the maximum output of the hybrid system [MW]; P_{MIN} is the minimum output of the hybrid system [MW]; and R is the variation range [MW].

- *Active power deviation W*

The active power deviation W is used to calculate the difference between the system active output power and the rated value. An increase in W reflects a greater deviation of the system output from the rated value:

$$W = \sum_{t=0}^{ts} \{P_{total}(t) - P_{ref}(t)\}^2 / N, \quad (2)$$

$$N = ts / \Delta t$$

where P_{total} is the active output power of the system [MW], P_{ref} is the reference output power [MW], t_s is the fluctuation time [s], Δt is the sample time [s], and N is the total number of samples.

- *Summation of peak and valley slopes α*

The summation of peak and valley slopes α shows the sum of the absolute values of the peak-valley slopes of the output power. An increase in α implies a stronger fluctuation of the hybrid system output:

$$\alpha = \sum_{t=0}^{ts} \left\{ \left| P_{total}(t) - P_{total}(t + \Delta t) \right| \right\} / ts, \quad (3)$$

where α is the summation of the peak and valley slopes.

2.3. Wind Turbine Model

A 1 MW permanent magnet-based direct-drive synchronous generator, coupled with a horizontal axis wind turbine, was considered for modelling. A combination of feedforward and fuzzy logic variable pitch control methods were applied and simulated, which is simple, effective, and robust.

2.3.1. Rotor Model

The power generated by airflow through a horizontal axis wind turbine is given as follows [28]:

$$Pr = Cp(\lambda, \beta) 0.5 \rho \pi R^2 V_W^3, \quad (4)$$

where Pr is the mechanical power generated by the WT [W]; Cp is the wind-power utilization coefficient [%; $Cp_{max} = 59\%$]; ρ is the density of air [g/L]; R is the radius of the WT blade [m]; V is the transverse wind velocity [m/s]; λ is the blade tip speed ratio; and β is the pitch angle.

The parameter λ was included since it is used in quantifying Cp, and is obtained from the following equation:

$$\lambda = \frac{\Omega R}{V}, \quad (5)$$

where Ω is the angular velocity of the rotor [rad/s].

The Cp of WTs are typically represented as a high-order polynomial of λ and β as follows:

$$Cp = \sum_{i=0}^4 \sum_{j=0}^4 c_{i,j} \beta^i \lambda^j, \quad (6)$$

where $c_{i,j}$ are coefficients.

In this study, the wind energy utilization coefficient Cp is calculated by the following empirical formula [29].

$$Cp = Cp(\beta, \lambda) = 0.22 \left[\frac{116}{\lambda_i} - 0.4\beta - 5 \right] e^{-\frac{12.5}{\lambda_i}} \quad (7)$$

$$\frac{1}{\lambda_i} = \frac{1}{\lambda + 0.08\beta} - \frac{0.035}{\beta^3 + 1}$$

2.3.2. Generator Model and Variable Pitch System

The generator is modelled as a permanent magnet synchronous generator using the PMSM module available in Simulink (a modelling software). A variable pitch system can be simulated by a first-order inertial system with delay, the transfer coefficient of which is obtained as follows [29]:

$$\frac{\beta(s)}{\beta_r(s)} = \frac{1}{T_\beta s + 1} e^{-\tau s}, \quad (8)$$

where T_β is the time constant [0.2]; β_r is the value at which the pitch angle is set; and τ is the time delay [0.1 s].

2.3.3. Control System Model

For wind speeds within the rated wind speed range of the turbine, the control system adjusts the pitch angle of the turbine blades to maintain a constant rotational speed, and thus a constant power output from the generator.

- Feedforward controller

The PMSM module adopted to model the generator does not include the electromagnetic and mechanical losses in the generator. The value of β in the feedforward controller is determined by fitting a curve in the plot of V versus β . Based on the above-mentioned empirical formula, considering the wind speed V as an input variable and the pitch angle β as an output variable, the following relation can be obtained [30]:

$$\beta = g[P_{WT}, V] = g[P_r, V]. \quad (9)$$

For the WT analyzed in this paper, the cut-in (V_{cut-in}) and cut-out ($V_{cut-out}$) speeds of the wind are 10 and 22 m/s. The flow chart in Figure 3a [30] shows the process for calculating the required pitch angle for wind speeds in the range from V_{cut-in} to $V_{cut-out}$ at intervals of 1 m/s. ε is a positive integer that represents the maximum allowable difference between the simulated wind power and a reference value, and is set at 1000. The calculated results are plotted in Figure 3b.

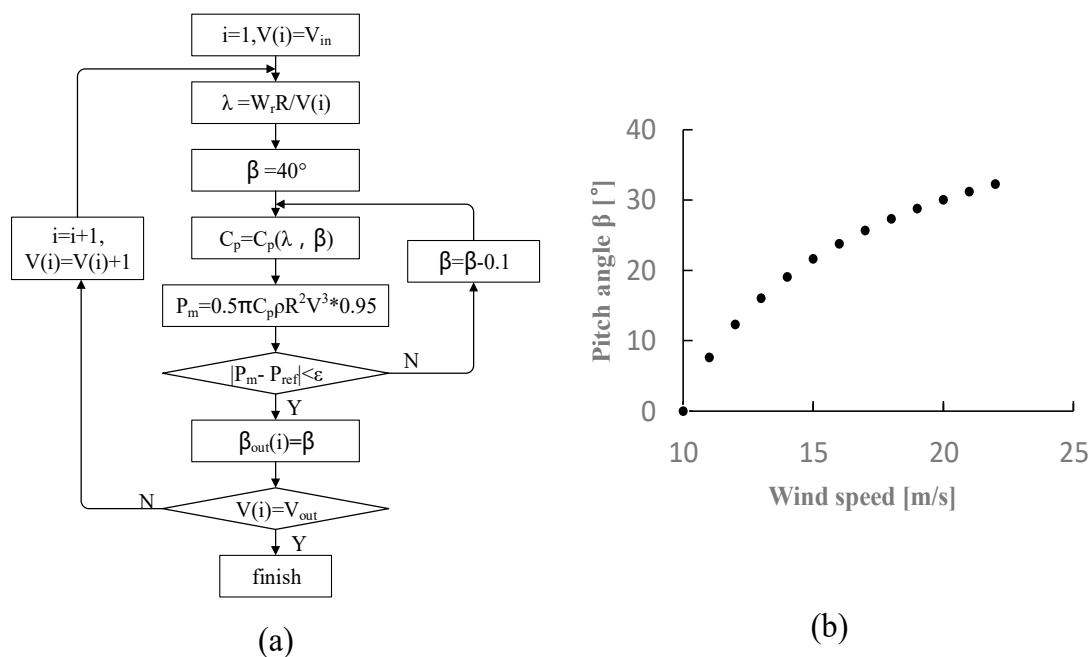


Figure 3. (a) Flow chart for the calculation of pitch angle; (b) calculated results.

The plot in Figure 3b shows a typical nonlinear relationship between wind speed and pitch angle. For convenience, the operating wind speed range was subdivided into three intervals: low: 10–14 m/s; medium: 14–18 m/s; and high: 18–22 m/s. The pitch angles at these three wind speed intervals are fitted by three separate third-order polynomials, and the value of the pitch angle at any given wind speed is obtained by querying these third-order polynomials. Based on the above study, the feedforward controller measures the wind speed and calculates the appropriate pitch angle.

- Fuzzy controller

The results of the previous calculations differ from the pitch angle required in practice. The feedforward controller is only capable of approximating the value of the pitch angle. It is necessary to

couple the feedforward controller with another control method that has a quick response, and can balance the relative error between the calculated result and the required pitch angle. To achieve this, a fuzzy-based controller is adopted for the optimal control of the WT system.

The fuzzy controller has several positive features, such as robustness, anti-jamming, and good control, when it is difficult to establish accurate mathematical models. There are four steps necessary for a fuzzy controller: establishing the knowledge base, fuzzification, fuzzy reasoning, and defuzzification. The established fuzzy domain and fuzzy subset are the basis of the knowledge base. The input value is fuzzified by a quantization factor. Fuzzy reasoning is then carried out using a rule table. Finally, the output of the fuzzy controller is de-fuzzified by a proportion factor.

The power error E and power error change rate E_c are the two inputs for the fuzzy-based controller. The outputs of the controller are the correction in the value of β , the basic domain of power error, and error change rate $[-10^5 W, 10^5 W]$, the basic domain of output $[-6^\circ, 6^\circ]$, and the quantization factor of 0.00006. The fuzzy domain of the output is $[-6^\circ, 6^\circ]$.

The fuzzy subset is $\{NM, NB, NS, PS, ZO, PB, PM\}$, the scale factor is 0.9, and the fuzzy rules are tabulated in Table 1 [30]. Defuzzification of the fuzzy subset is processed using the centroid of gravity method.

Table 1. Fuzzy rule table for the controller.

$E_c \backslash E$	(NB)	(NM)	(NS)	(ZO)	(PS)	(PM)	(PB)
(NB)	(PB)	(PB)	(PB)	(PM)	(PS)	(ZO)	(ZO)
(NM)	(PM)	(PM)	(PM)	(PS)	(PS)	(ZO)	(ZO)
(NS)	(PM)	(PS)	(PS)	(PS)	(ZO)	(ZO)	(ZO)
(ZO)	(PS)	(PS)	(PS)	(ZO)	(NS)	(NS)	(NS)
(PS)	(ZO)	(ZO)	(ZO)	(NS)	(NS)	(NS)	(NM)
(PM)	(ZO)	(ZO)	(NS)	(NS)	(NM)	(NM)	(NM)
(PB)	(ZO)	(ZO)	(NS)	(NM)	(NB)	(NB)	(NB)

Thus, when the wind speed changes, the fuzzy controller tracks the deviation between the output and the required setting value of the pitch angle, and corrects it to achieve a constant power operation for the WT. Based on the above analysis, a complete variable pitch controller model for the WT is shown as follows in Figure 4.

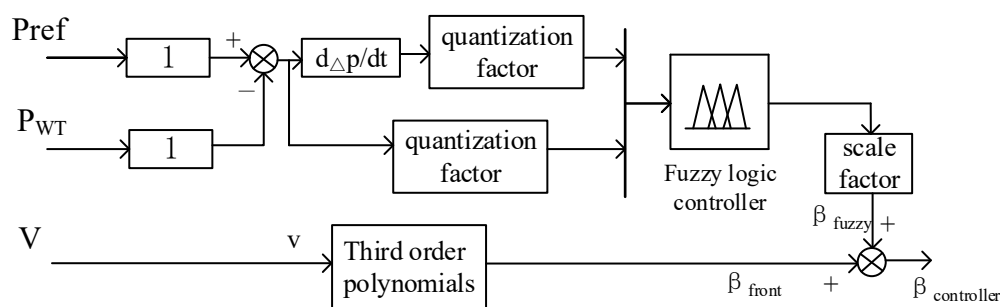


Figure 4. Fuzzy feedforward controller model for a wind turbine.

2.3.4. Wind Turbine Model Simulation

The output value of the pitch angle, active power, and rotational speed of the WT are measured, for an initial wind speed range of 10 to 22 m/s, varied at 1 m/s over a time interval of 10 s, followed

by a wind speed range of 22 to 10 m/s at the same rate of change of wind speed. The results are as depicted in Figure 5.

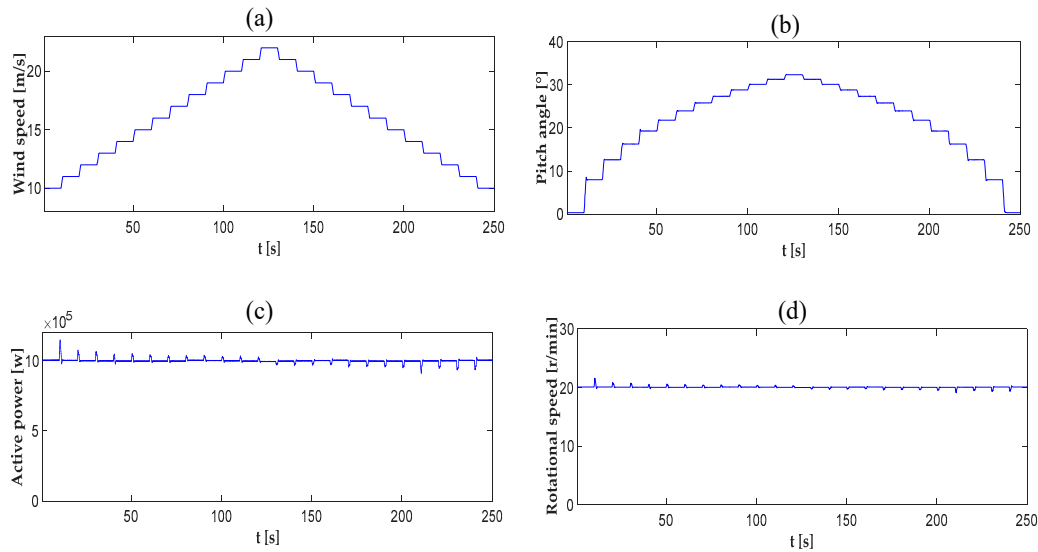


Figure 5. (a) Stepped wind; (b) Output value of pitch angle; (c) WT output active power; (d) Rotational speed of WT.

From the fuzzy feedforward controller, the pitch angle and wind speed follow a non-linear relationship. The resulting WT output has a short adjustment time, less overshoot, and a constant rotational speed and power.

2.4. Photo-Voltaic Model

A practical solar cell model is adopted in this paper, and the output characteristics of solar arrays are simulated for different solar radiation intensities.

2.4.1. Solar Cell Model

Barring certain minor factors [31], the simulation model of a silicon solar cell is equivalent to that of a mathematical model of a universal solar cell. In this section, the mathematical expressions of the simulation model of a solar cell are obtained as follows [31]:

$$\begin{aligned}
 C_1 &= \left(1 - \frac{I_m}{I_{sc}}\right) \exp\left(-\frac{V_m}{C_2 V_{oc}}\right) \\
 C_2 &= \left(\frac{V_m}{V_{oc}} - 1\right) / \ln\left(1 - \frac{I_m}{I_{sc}}\right) \\
 T_1 &= T - T_{ref} \\
 S_1 &= \frac{S}{S_{ref}} - 1 \\
 D &= I_{sc} S_1 + a T_1 (1 + S_1) \\
 dv &= b T_1 + D R_s \\
 I &= I_{sc} \left\{1 - C_1 \left[1 - \exp\left(\frac{V+dv}{C_2 V_{oc}}\right)\right]\right\} + D
 \end{aligned} \tag{10}$$

where I_{sc} is the short-circuit current [4.75 A]; V_{oc} is the open-circuit voltage [21.75 V]; I_m is the current at maximum power [4.515 A]; V_m is the voltage at maximum power [17.25 V]; T_{ref} is the operating temperature; S_{ref} is the reference value of the illumination intensity; C_1 , C_2 , T_1 , and S_1 are intermediate variables; a , b are compensation factors [$a = 0.0054$, $b = 0.21$]; S is the solar radiation intensity; and T is the battery temperature.

2.4.2. Photo-Voltaic Model Simulation

Silicon solar cells were modelled and simulated based on the above formulas. Considering the I–V (current flow versus voltage across the solar cell) and P–V (output active power versus voltage across the solar cell) curves of PV systems at a temperature of 25 °C, the solar radiation intensities of 1000, 800, 600, 400, and 200 W/m² are depicted in Figures 6 and 7.

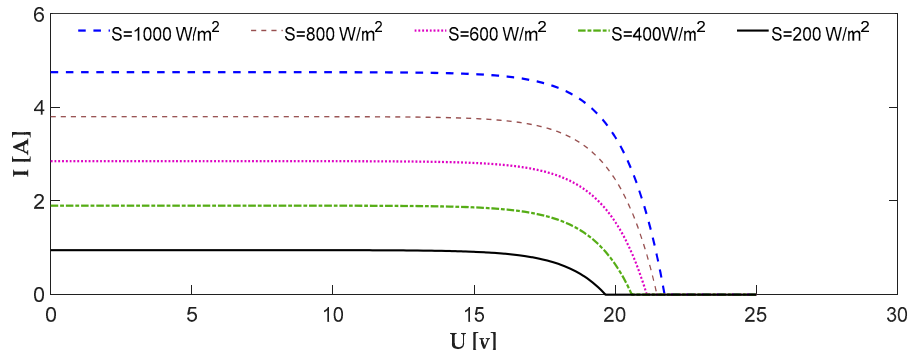


Figure 6. I–V (current flow versus voltage) curves of photovoltaic cells at T = 25 °C.

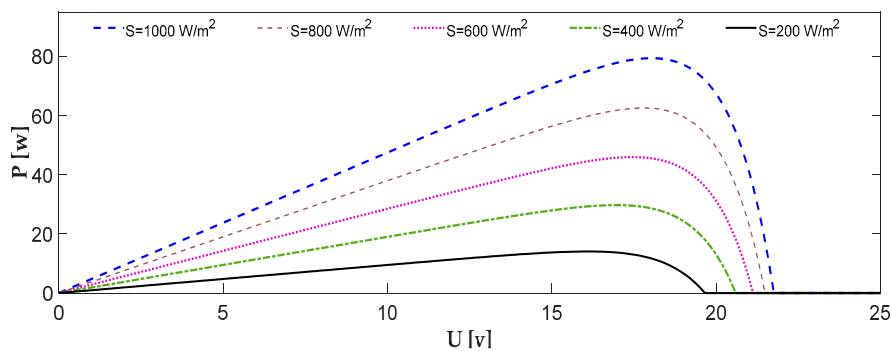


Figure 7. P–V (output active power versus voltage) curves of photo-voltaic cells at T = 25 °C.

According to the I–V and P–V curves of photo-voltaic cells, the output current of photo-voltaic cells remains constant as the voltage increases, while the output power increases to the maximum value. As the voltage continues to increase, the output power and current decrease from the maximum values to zero. In this article, considering a reference temperature T_{ref} of 25 °C and a voltage of 18 V, the maximum output power from the photovoltaic cells is obtained, and this working condition is subsequently adopted.

2.5. Hydro Turbine Model

A hydropower unit has relatively quick and flexible start and stop power generation characteristics, and can hence become operational from an idle state within a few minutes. The load increase and decrease tasks can be completed in a short time and the load can be varied over a wide range. In this work, a 50 MW hydro turbine including a pressure penstock is introduced to compensate for the power fluctuations derived from wind and solar energy.

2.5.1. Electro-Hydraulic Servo System Model

In a dynamic process with large fluctuations, the linear part of the transfer function of the electro-hydraulic servo system is expressed as [32]:

$$G(s) = \frac{Y(s)}{Y_{PID}(s)} = \frac{1}{T_y s + 1}, \quad (11)$$

where Y_{PID} is the governor output, Y is the guide vane opening, and T_y is the servomotor response time constant.

In a mechanical hydraulic system, the full-stroke closing time T_f and the full-stroke opening time T_g of the two-stage closing characteristics of a servomotor are considered. T_f is the minimum time required for the servo to close from being 100% open to being fully closed, and this is limited by the maximum closing speed of the relay. T_g is the minimum time required for the servomotor to open from being fully closed to being 100% open, and this is limited by the maximum opening speed of the servo, which is controlled by the rate limiter module. Additionally, the working stroke of the servomotor changes from fully closed to fully open, and this is controlled by a saturation module.

2.5.2. Pressure Penstock and Hydro-Turbine Model

The penstock system with elastic water hammer is presented with its transfer function, which is expressed as [33]:

$$G_h(s) = \frac{H(s)}{Q(s)} = -h_w \frac{T_r s + \frac{1}{24} T_r^3 s^3}{1 + \frac{1}{8} T_r^2 s^2}, \quad (12)$$

where H is the water head, Q is the hydro-turbine flow, h_w is the pipeline characteristic coefficient, and T_r is the time constant of the elastic water hammer.

The transfer function of hydro-turbine can be written as [34]:

$$G_t(s) = \frac{M_t(s)}{Y(s)} = e_y \frac{1 + e G_h(s)}{1 - e_{qh} G_h(s)}, \quad (13)$$

where M_t is the hydro-turbine mechanical torque, e_y is the transfer coefficient of the mechanical torque M_t to the guide vane opening Y , e_{qh} is the transfer coefficient of the water flow Q to the water head H , e_{qy} is the transfer coefficient of the water flow Q to the guide vane opening Y , and e_{mh} is transfer coefficient of the mechanical torque M_t to the water head H .

According to Equations (9) and (10), we can model the pressure penstock and hydro-turbine by considering the elastic water hammer as:

$$G_t(s) = e_y \frac{24 - 24e h_w T_r s + 3T_r^2 s^2 - e h_w T_r^3 s^3}{24 + 24e_{qh} h_w T_r s + 3T_r^2 s^2 + e_{qh} h_w T_r^3 s^3}. \quad (14)$$

2.5.3. Generator and Load Model

The generator load transfer function is a first-order inertial system:

$$G_g(s) = \frac{X(s)}{M(s)} = \frac{1}{T_a s + e_n}, \quad (15)$$

where X is the hydro-turbine generator rotational speed, M is the hydro-turbine generator mechanical torque difference, T_a is the inertial time constant, and e_n is the comprehensive self-regulation coefficient of the hydro-turbine generator.

2.5.4. Governor

The governor is the core element required for the stable operation of a hydro turbine-generator system. It has three main adjustment modes, including the frequency adjustment mode, the opening adjustment mode, and the power adjustment mode. In this design, the PID (Proportional Integral Derivative) controller is considered and the control diagram is presented in Figure 8 [32].

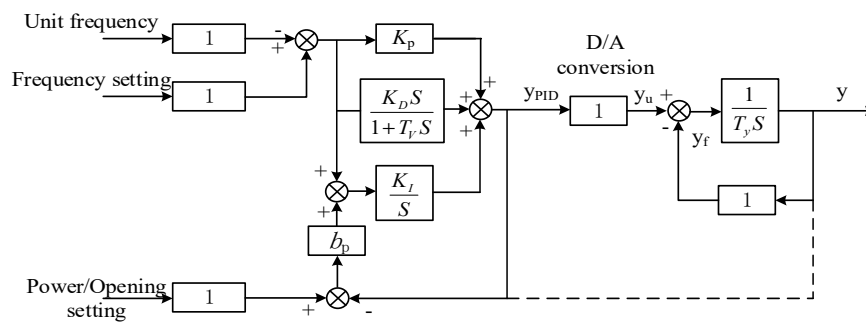


Figure 8. PID controller for the governor.

3. Complementary Feasibility Analysis

For an optimal coordinated operation in a hybrid system, the short-term wind flow uncertainty and solar radiation variation must be considered. In complementary hybrid power generation systems, hydropower generation can make up for the shortcomings of various intermittent renewable energy sources, by rapidly offsetting output power fluctuations. In this section, with reference to the wind power national standard, the influence of the short-term fluctuations of the wind power is considered, and the necessity of hydro turbine regulation under various wind fluctuations is analyzed. In the same way, the short-term fluctuation of the solar energy generator is analyzed.

3.1. Effect of Wind Fluctuations on the Power Characteristics of a WT

Short-term fluctuations of wind speed impact the output power of a WT. The resulting small fluctuations in outpower can disappear rapidly with a variable pitch control system, but the impact of wind fluctuation does not disappear rapidly under the following two circumstances:

- With a sudden rise or fall in wind turbulence, the output torque of the wind turbine changes rapidly due to a series of mechanical or electrical delays, which lead to large fluctuations in the output power of the system over a short time interval.
- When the wind speed exceeds $V_{cut-out}$ or becomes lower than V_{cut-in} , the active power output becomes zero.

From the above analysis, five types of wind speed fluctuations are considered in this work as shown in Figure 9. These is the sudden rise or fall of wind speed from low to medium (12–16 m/s), medium to high (16–20 m/s), high to medium (20 m/s–16 m/s), and medium to low (16–12 m/s). After 300 s of simulation, the wind speed falls gradually below V_{cut-in} . For a WT installed capacity of 1 MW–5 MW, the system active power output for five wind speed fluctuations is presented in Figure 10.

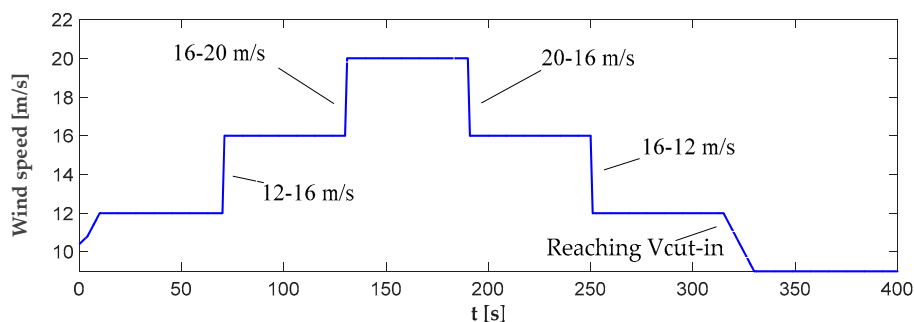


Figure 9. Five types of short-term interval wind fluctuations.

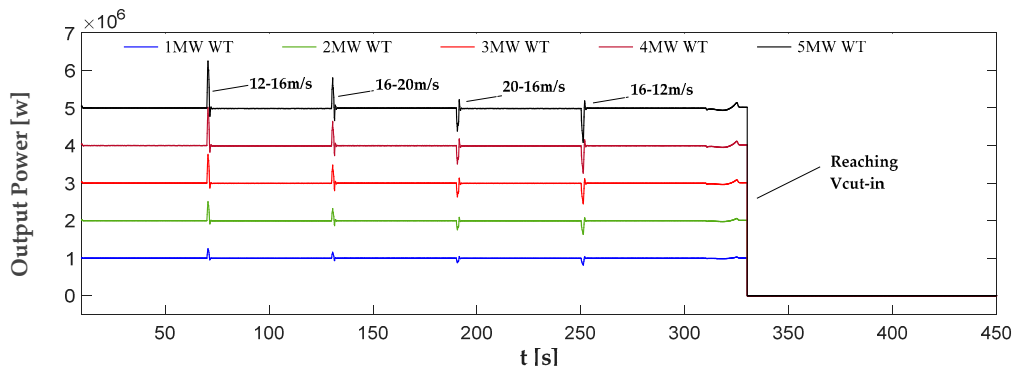


Figure 10. Active power output of WT with five installed capacity of 1–5 MW under five different wind fluctuations.

For a constant power WT, it is seen that a sudden rise or fall in wind speed causes output to overshoot in a short time interval. Besides, a sudden change of wind speed at a low wind speed has a greater impact on the output than that at a high wind speed. After 300 s, as the wind speed reaches v_{cut-in} , and the active power drops to zero.

3.2. Feasibility Analysis of WT-HT complementarity

This paper refers to the regulation of the maximum value of active power deviation of a wind farm under normal operation: for a wind power generation system with an installed capacity of less than 30 MW, the power deviation is 3 MW at its maximum output, over a one-minute time interval.

In the WT-HT hybrid system, the wind turbine output is evaluated in Figure 10 by the proposed indicators t_s and R . When a certain wind speed fluctuation leads to the wind turbine output being beyond the standard, hydro turbine regulation will be adopted.

For a sudden rise or fall in wind speed, R less than 3 MW, and a short duration of fluctuation of wind speed, the influence on the output of WT is for a short duration, and hence complementary adjustments by HT in the hybrid system are not necessary. However, for R larger than 3 MW, a complementary adjustment is needed. If the wind does not reach the rated speed and the WT has no active power output, then the hybrid system requires the HT to operate small wave transforms that quickly offset the power loss. Based on Figure 9 and the above assessment methods, the results of the feasibility analysis of WT-HT complementarity with five types of wind fluctuation are presented in Table 2.

Table 2. Analysis of the complementary feasibility of the WT-HT (wind turbine-hydro turbine) hybrid system with WT capacity of 1 MW–5 MW under the influence of wind fluctuations (N-without complementary adjustment by HT; Y-with complementary adjustment by HT; O-needs further study).

Capacity	Fluctuation	12–16 m/s		16–20 m/s		20–16 m/s		16–12 m/s		Reach V_{cut-in}	
		R/MW	Result	R/MW	Result	R/MW	Result	R/MW	Result	R/MW	Result
1 MW		0.301	N	0.229	N	0.169	N	0.222	N	1	Y
2 MW		0.602	N	0.457	N	0.338	N	0.443	N	2	Y
3 MW		0.903	N	0.686	N	0.507	N	0.664	N	3	Y
4 MW		1.204	N	0.915	N	0.675	N	0.886	N	4	Y
5 MW		1.505	N	1.143	N	0.844	N	1.107	N	5	Y

3.3. Effects of Solar Radiation Fluctuation on the Power Characteristics of PV Systems

Photovoltaic output is greatly affected by weather. Rainy and cloudy days are the leading cause of system output fluctuations, with fluctuations occasionally exceeding 50% of the installed capacity of the PV system.

As mentioned in prior research, on a time scale of 1 min, a logistic distribution is best suited to fit photovoltaic output fluctuations. On a time scale of 2–60 min, a t-location scale distribution is more appropriate to fit photovoltaic output fluctuations.

The fluctuations of solar radiations lead to fluctuations in photovoltaic output, and the change in power output is the same as that of photovoltaic output. In this paper, three time steps of fluctuations of solar radiation are considered and modelled: 1, 2, and 10 min, and the effects of 50% and 100% fluctuations on photovoltaic output for these three time scales are considered. In Figure 11a,b, six types of solar radiation fluctuations are plotted; and the active power outputs for PV systems with installed capacities in the range of 1–5 MW are presented in Figure 11c,d.

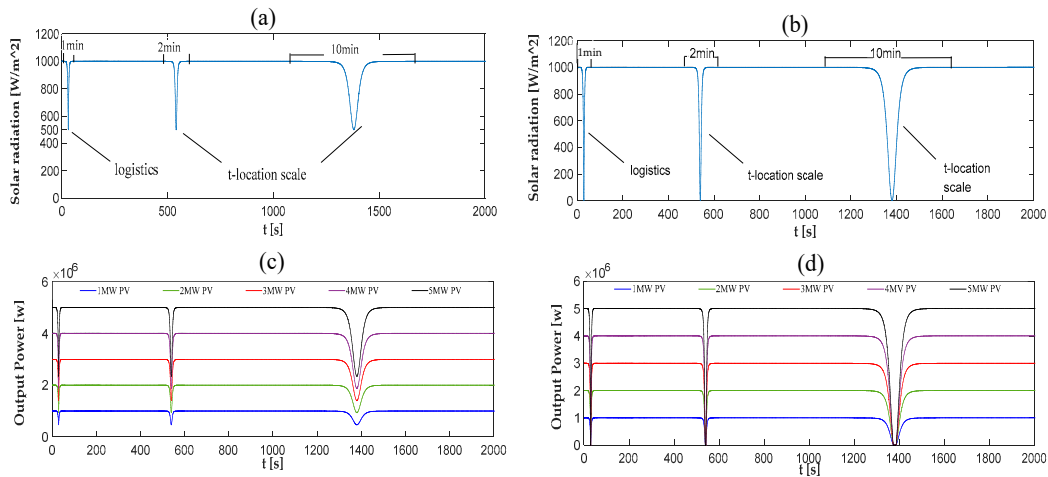


Figure 11. (a) 50% solar radiation fluctuation in 1-, 2-, and 10-min intervals (b) 100% solar radiation fluctuations in 1-, 2-, and 10-min intervals (c,d) active power output of PV with installed capacities of 1–5 MW.

From Figure 11c,d, with regard to the three types of fluctuations of solar radiation, it is seen that the obtained output power variation ranges are the same. With 50% solar radiation fluctuations, the output of the PV system fluctuated by more than 50%. With 100% solar radiation fluctuations, and when solar radiation is lower than 61 W/m², the output of PV drops to zero.

3.4. Feasibility Analysis of PV-HT Complementarity

This paper refers to the technical regulations on grid-connected photovoltaic volatility in national grid-connection standards: the maximum deviation in active power over a 10-min interval is 10 MW, and the maximum deviation of active power in 1 min is 3 MW.

The evaluation method is the same as the WT, and the influence of solar radiation fluctuation on PV output under three time steps is analyzed in Table 3.

Table 3. Analysis of the complementary feasibility of the PV-HT (photovoltaics-hydro turbine) hybrid system with PV capacity of 1 MW–5 MW under the influence of solar radiation fluctuation (N-without complementary adjustment by HT; Y-with complementary adjustment by HT; O-needs further study).

Capacity	Fluctuation	50%flu (1 min, 2 min, 10 min)		100%flu (1 min, 2 min, 10 min)	
		R/MW	Analysis	R/MW	Analysis
1 MW		0.532	○	0.229	○
2 MW		0.602	○	0.457	○
3 MW		0.903	○	0.686	Y
4 MW		1.204	○	0.915	Y
5 MW		1.505	○	1.143	Y

For a 100% fluctuation of solar radiation over these three time intervals, it is necessary to activate the hydraulic turbine for complementary adjustment when the installed capacity of PV ranges from 3–5 MW. However, for the other cases mentioned in this paper, the fluctuation of the PV output does not meet the required conditions for regulation. Given that the fluctuation of solar radiation has a long influence time, and that no previous research has been conducted at this working condition, the necessity of complementary adjustment using hydropower needs to be addressed.

4. Assessment Results

4.1. Combined Operation of a Wind Turbine and a Hydro Turbine

According to the analysis of the previous chapter, for sudden increases and decreases in the wind speed of a WT-HT hybrid system, it is unnecessary to utilize complementary adjustment by hydraulic turbines. When the wind speed is lower than v_{cut-in} , the complementary adjustment is needed. For five types of wind fluctuations, the simulation output is depicted in Figure 12, and the evaluation of the WT-HT hybrid system output with the above-mentioned indicators is shown in Table 4.

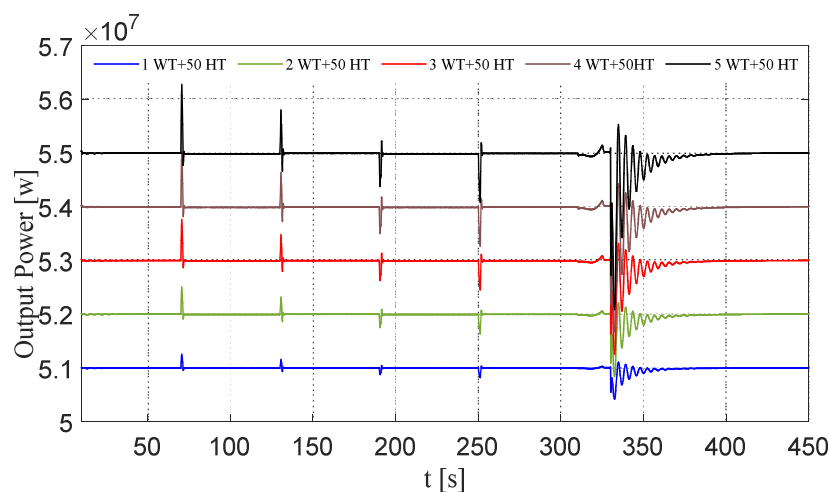


Figure 12. Output power of the WT-HT hybrid system with a WT installed capacity of 1–5 MW under five types of wind fluctuations.

Table 4. Assessment results for a WT-HT hybrid system.

		Fluctuation Time [s]					Active Power Range [MW]				
		1 min 50%flu	1 min 50%	20–16 m/s	16–12 m/s	Reach Vcut-in	12–16 m/s	16–20 m/s	20–16 m/s	16–12 m/s	Reach Vcut-in
Capacity	1 MW	20	3	3	3	38	0.301	0.229	0.169	0.222	0.68
	2 MW	20	3	3	3	41	0.602	0.457	0.338	0.443	1.37
	3 MW	3	3	3	3	44	0.903	0.686	0.507	0.664	2.06
	4 MW	3	3	3	3	47	1.204	0.915	0.675	0.886	2.75
	5 MW	3	3	3	3	50	1.505	1.143	0.844	1.107	3.45
		Active Power Deviation					Summation of Peak and Valley Slopes				
		12–16 m/s	16–20 m/s	20–16 m/s	16–12 m/s	Reach Vcut-in	12–16 m/s	16–20 m/s	20–16 m/s	16–12 m/s	Reach Vcut-in
Capacity	1 MW	0.012	0.002	0.003	0.008	0.024	0.2	0.165	0.128	0.147	0.101
	2 MW	0.048	0.017	0.011	0.031	0.09	0.401	0.329	0.256	0.294	0.188
	3 MW	0.109	0.038	0.025	0.069	0.189	0.602	0.494	0.384	0.441	0.264
	4 MW	0.193	0.067	0.045	0.123	0.315	0.803	0.659	0.512	0.588	0.331
	5 MW	0.302	0.105	0.071	0.192	0.463	1.004	0.824	0.64	0.735	0.39

With an increase in the WT installed capacity, the influence of short-term wind speed fluctuations on the output of the WT-HT hybrid system is important to consider. In the analysis of a sudden rise and fall in wind speed, it is observed that the impact of low wind speed on the hybrid system output is stronger than that for a high wind speed, and the degree of impact on the system is “12–16 m/s” > “16–12 m/s” > “16–20 m/s” > “20–16 m/s”. As the wind speed reaches v_{cut-in} , the hybrid system output oscillates for a certain amount of time.

In terms of fluctuation time, the impact of all sudden increases and decreases in wind speed on the hybrid system are for 3 s. When the wind speed is lower than v_{cut-in} , with an increase in the WT installed capacity from 1 to 5 MW, the time taken for the complementary adjustment of hydraulic turbines to restore the stability of the system increases from 38 to 50 s, which is higher than the impact of a sudden rise and fall of wind speed fluctuation.

The three indicators to evaluate the influence of five types of wind speed fluctuations on hybrid systems, when comparing “reached v_{cut-in} ” and “12–16 m/s” conditions, are: the variation range of the former is about 2.3 times that of the latter, the active power deviation of the former is about 1.5–2 times that of the latter and the ratio drops with an increase in the installed capacity of the WT, and the active power fluctuation of the former is about 0.4–0.5 times that of the latter and the ratio drops with an increase in the installed capacity of the WT.

4.2. Combined Operations of Photovoltaic and Hydro Turbine Systems

According to the analysis of the previous chapter, for a 50% fluctuation of solar radiation intensity in PV systems with an installed capacity of 1 MW–5 MW, it is as yet undetermined as to whether a complementary adjustment with a hydraulic turbine is necessary. For a 100% fluctuation in 1–3 MW installed capacity of PV systems, the need for a complementary adjustment also remains undetermined. For PV-HT hybrid systems with PV installed capacities of 4 and 5 MW, complementary adjustments using hydraulic turbines are needed, as shown by the simulation results in Figures 13 and 14.

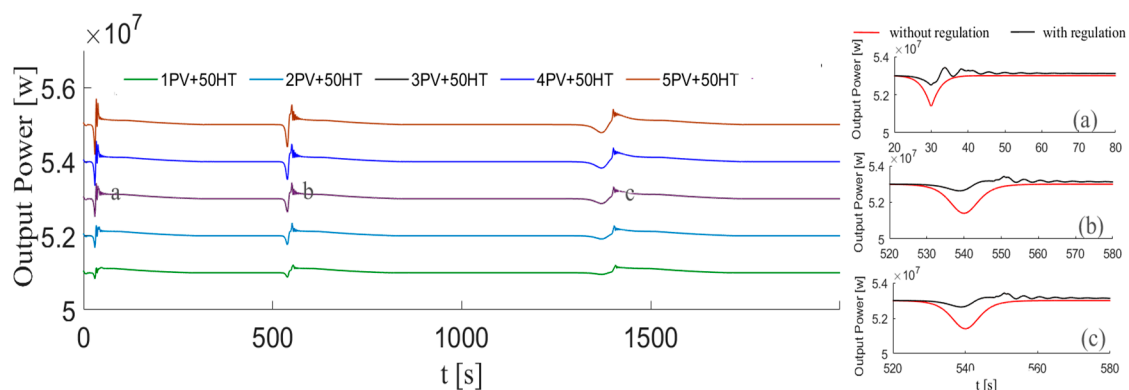


Figure 13. Output power of a PV-HT hybrid system with 50% solar radiation fluctuation, for fluctuation times of 1, 2, 10 min; (a–c) are the comparisons of output power with and without hydro turbine regulation of a 3 MW photovoltaic system.

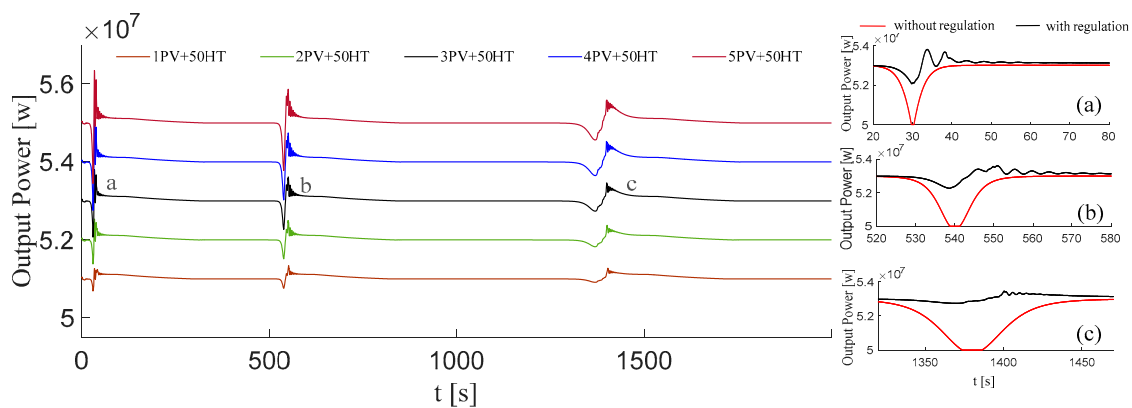


Figure 14. Output power of a PV-HT hybrid system with 100% solar radiation fluctuation, for fluctuation times of 1, 2, and 10 min; (a–c) are the comparisons of output power with and without hydro turbine regulation of a 3 MW photovoltaic system.

In Figures 13 and 14, the results of the participation of a hydro turbine in the regulation of a 3 MW photovoltaic system are presented, and compared with the output without regulation. For six types of solar radiation fluctuations, the PV-HT hybrid system output was evaluated with the above-mentioned indicators as shown in Tables 5 and 6.

When solar radiation fluctuation occurs, and the hydraulic turbine is not adopted for complementary adjustments, radiation fluctuations for 1, 2, and 10 min lead to power output fluctuations for 20, 40, and 200 s. For 50% solar radiation fluctuation, with the hydraulic turbine used for complementary adjustments, the radiation fluctuations for 1, 2, and 10 min increase the respective system adjustment time by 4–6, 3–3.5, and 1.1–1.3 times, and the ratio rises with increased PV installed capacity. For 100% solar radiation fluctuation, the respective adjustment time increases 14–16, 7–8, and 2–2.2 times, for each time interval, and the ratio also rises with increased PV installed capacity. Compared with non-complementary regulation, adding HT regulation will increase the adjustment time of hybrid systems under short-term external disturbances, and the stronger or quicker the disturbance, the longer the time required to restore stability.

The range of active power variation, output deviation, and extent of fluctuation of the hybrid system, with hydraulic turbines participating in regulation, are greatly decreased. Considering the three indicators, the 100% fluctuation has a greater impact on system output than the 50% fluctuation, and a one-minute fluctuation has a greater impact on the system output than fluctuations for 2 and 10 min. The larger the fluctuation range of solar radiation intensity or the shorter the fluctuation time, the greater the impact on the output of the system.

Table 5. Assessment results for a PV-HT hybrid system with 50% solar radiation fluctuation.

		Fluctuation Time [s]						Active Power Range [MW]					
Capacity	Fluctuation	1 min	1 min	2 min	2 min	10 min	10 min	1 min	1 min	2 min	2 min	10 min	10 min
		50%	50% (fix)	50%	50% (fix)	50%	50% (fix)	50%	50% (fix)	50%	50% (fix)	50%	50% (fix)
	1 MW	20	93	40	122	190	234	0.532	0.031	0.532	0.033	0.532	0.025
	2 MW	20	100	40	129	190	241	1.065	0.061	1.065	0.058	1.065	0.036
	3 MW	20	110	40	135	190	251	1.597	0.091	1.597	0.08	1.597	0.045
	4 MW	20	115	40	138	190	258	2.129	0.121	2.129	0.097	2.129	0.055
	5 MW	20	118	40	141	190	261	2.661	0.152	2.661	0.115	2.661	0.064
		Active Power Deviation						Summation of Peak and Valley Slopes					
Capacity	Fluctuation	1 min	1 min	2 min	2 min	10 min	10 min	1 min	1 min	2 min	2 min	10 min	10 min
		50%	50% (fix)	50%	50% (fix)	50%	50% (fix)	50%	50% (fix)	50%	50% (fix)	50%	50% (fix)
	1 MW	0.037	0.011	0.048	0.012	0.051	0.008	0.042	0.011	0.022	0.007	0.005	0.003
	2 MW	0.15	0.017	0.194	0.016	0.205	0.012	0.085	0.02	0.045	0.012	0.01	0.004
	3 MW	0.338	0.024	0.435	0.023	0.46	0.015	0.127	0.027	0.067	0.018	0.016	0.005
	4 MW	0.608	0.031	0.771	0.003	0.818	0.019	0.171	0.031	0.09	0.022	0.021	0.006
	5 MW	0.938	0.041	1.211	0.038	1.278	0.023	0.212	0.036	0.113	0.025	0.026	0.007

Table 6. Assessment results for a PV-HT hybrid system with 100% solar radiation fluctuation.

		Fluctuation Time [s]						Active Power Range [MW]					
Capacity	Fluctuation	1 min	1 min	2 min	2 min	10 min	10 min	1 min	1 min	2 min	2 min	10 min	10 min
		100%	100% (fix)	100%	100% (fix)	100%	100% (fix)	100%	100% (fix)	100%	100% (fix)	100%	100% (fix)
	1 MW	20	283	40	288	190	399	1	0.058	1	0.058	1	0.036
	2 MW	20	293	40	295	190	415	2	0.115	2	0.099	2	0.055
	3 MW	20	299	40	302	190	425	3	0.173	3	0.134	3	0.072
	4 MW	\	303	\	306	\	436	\	0.231	\	0.172	\	0.088
	5 MW	\	309	\	312	\	440	\	0.289	\	0.208	\	0.103
		Active Power Deviation						Summation of Peak and Valley Slopes					
Capacity	Fluctuation	1 min	1 min	2 min	2 min	10 min	10 min	1 min	1 min	2 min	2 min	10 min	10 min
		100%	100% (fix)	100%	100% (fix)	100%	100% (fix)	100%	100% (fix)	100%	100% (fix)	100%	100% (fix)
	1 MW	0.154	0.017	0.189	0.016	0.198	0.011	0.079	0.018	0.042	0.012	0.01	0.004
	2 MW	0.623	0.032	0.748	0.03	0.794	0.018	0.159	0.031	0.084	0.022	0.02	0.006
	3 MW	1.385	0.05	1.692	0.047	1.784	0.027	0.237	0.041	0.127	0.03	0.029	0.008
	4 MW	\	0.078	\	0.07	\	0.038	\	0.054	\	0.036	\	0.01
	5 MW	\	0.111	\	0.098	\	0.051	\	0.069	\	0.043	\	0.012

5. Conclusions

The paper enriches the existing framework, departs from the norm of using an hour as the minimum time scale for a theoretical framework, and explored the operational characteristics of hybrid systems over short time intervals. Based on the classic models of wind, solar, and hydro generation units, the necessity of hydraulic turbine regulation for short-term fluctuations of wind and solar energy was studied. Finally, the output of the hybrid system was evaluated and the stability of the system under various short-term fluctuations was analyzed.

When the wind speed reaches v_{cut-in} , the hydraulic turbine complementary regulation is deployed in the model, which leads to a long adjustment time of the WT-HT hybrid system. The larger the installed capacity of the WT, the greater the regulating effect of the hydraulic turbine. When the effects of different wind speed fluctuations on the hybrid system are compared, it is observed that the adjustment time required for the wind speed v_{cut-in} leads to a greater variation range and deviation of the active power output, while the sudden rise and fall of wind speed leads to a stronger fluctuation of the system.

For short durations of solar radiation fluctuations, complementary regulation by a hydraulic turbine system results in controlling power output fluctuations to a greater extent. The stronger the intensity of solar radiation fluctuation, the greater the complementary effect.

Concentrating on the hybrid system's stability, the proposed method showed a good performance in analyzing the short and sharp fluctuation of wind and solar energy. However, this method cannot solve the condition that the wind and solar power fluctuations exceed the hydropower regulation capacity by 20%, which is the focus in the next study. In addition, the economic index of the system is not included in this paper, which will be discussed later to enrich the established evaluation system. For the above discussion, the follow-up research programs are as follows: the system stability on a time scale of seconds, the load traceability on a time scale of an hour, and the economic efficiency on a time scale of a day will be considered systematically. The analysis of the three time scales are correlated and also independent of each other. For the three time scales, the energy utilization rate, electricity expectation ratio, and other indicators are employed, and a multi-time scale model of hybrid systems is established, which is of significance as a reference in the construction of multi-energy complementary projects.

Author Contributions: T.Z.: Conceptualization, Methodology, Investigation, Software, Formal analysis, Data curation, Visualization, Writing—original draft, Writing—review and editing. D.C.: Conceptualization, Methodology, Project administration, Supervision, Resources. J.L.: Software, Investigation, Methodology, Writing—original draft. B.X.: Software, Supervision. V.M.: Supervision, Writing—review and editing. All authors have read and agreed to the published version of the manuscript.

Funding: This work was funded by the Natural Science Foundation of Shaanxi Province (2019JLP-24). Shaanxi Science and Technology Co-ordination and Innovation Project of China (2020TD-025).

Acknowledgments: This work is supported by the Natural Science Foundation of Shaanxi Province (2019JLP-24), Shaanxi Science and Technology Co-ordination and Innovation Project of China (2020TD-025).

Conflicts of Interest: The authors declare no conflict of interest.

References

1. Hopkins, A.S. Burn Out The Endgame for Fossil Fuels. *Science* **2017**, *356*, 709. [[CrossRef](#)] [[PubMed](#)]
2. Lund, H. Renewable energy strategies for sustainable development. *Energy* **2007**, *32*, 912–919. [[CrossRef](#)]
3. Huda, M.; Koji, T.; Aziz, M. Techno economic analysis of vehicle to grid (V2G) integration as distributed energy resources in Indonesia power system. *Energies* **2020**, *13*, 1162. [[CrossRef](#)]
4. Halasz, G.; Malachi, Y. Solar energy from Negev desert, Israel: Assessment of power fluctuations for future PV fleet. *Energy Sustain. Dev.* **2014**, *21*, 20–29. [[CrossRef](#)]
5. Ramirez, F.J.; Honrubia-Escribano, A.; Gomez-Lazaro, E.; Pham, D.T. The role of wind energy production in addressing the European renewable energy targets: The case of Spain. *J. Clean. Prod.* **2018**, *196*, 1198–1212. [[CrossRef](#)]

6. Jo, K.H.; Kim, M.K. Stochastic Unit Commitment Based on Multi-Scenario Tree Method Considering Uncertainty. *Energies* **2018**, *11*, 740. [[CrossRef](#)]
7. Paish, O. Small hydro power: Technology and current status. *Renew. Sustain. Energy Rev.* **2002**, *6*, 537–556. [[CrossRef](#)]
8. Li, H.H.; Chen, D.Y.; Zhang, H.; Wu, C.Z.; Wang, X.Y. Hamiltonian analysis of a hydro-energy generation system in the transient of sudden load increasing. *Appl. Energy* **2017**, *185*, 244–253. [[CrossRef](#)]
9. Mitani, T.; Aziz, M.; Oda, T.; Uetsuji, A.; Watanabe, Y.; Kashiwagi, T. Annual assessment of large-scale introduction of renewable energy: Modeling of unit commitment schedule for thermal power generators and pumped storages. *Energies* **2017**, *10*, 738. [[CrossRef](#)]
10. Scarabaggio, P.; Carli, R.; Cavone, G.; Dotoli, M. Smart Control Strategies for Primary Frequency Regulation through Electric Vehicles: A Battery Degradation Perspective. *Energies* **2020**, *13*, 4586. [[CrossRef](#)]
11. Koroneos, C.; Dompros, A.; Roumbas, G. Renewable energy driven desalination systems modelling. *J. Clean. Prod.* **2007**, *15*, 449–464. [[CrossRef](#)]
12. Jacobson, M.Z. Roadmaps to Transition Countries to 100% Clean, Renewable Energy for All Purposes to Curtail Global Warming, Air Pollution, and Energy Risk. *Earths Future* **2017**, *5*, 948–952. [[CrossRef](#)]
13. Zhang, P.D.; Yang, Y.L.; Shi, J.; Zheng, Y.H.; Wang, L.S.; Li, X.R. Opportunities and challenges for renewable energy policy in China. *Renew. Sustain. Energy Rev.* **2009**, *13*, 439–449.
14. Takata, G.; Katayama, N.; Miyaku, M.; Nanahara, T. Study on power fluctuation characteristics of wind energy converters with fluctuating turbine torque. *Electr. Eng. Jpn.* **2005**, *153*, 1–11. [[CrossRef](#)]
15. Prasad, A.A.; Taylor, R.A.; Kay, M. Assessment of solar and wind resource synergy in Australia. *Appl. Energy* **2017**, *190*, 354–367. [[CrossRef](#)]
16. Idehen, I.; Abraham, S.; Murphy, G.V. A Method for Distributed Control of Reactive Power and Voltage in a Power Grid: A Game-Theoretic Approach. *Energies* **2018**, *11*, 962. [[CrossRef](#)]
17. Ardizzon, G.; Cavazzini, G.; Pavesi, G. A new generation of small hydro and pumped-hydro power plants: Advances and future challenges. *Renew. Sustain. Energy Rev.* **2014**, *31*, 746–761. [[CrossRef](#)]
18. Liu, Z.F.; Zhang, Z.; Zhuo, R.Q.; Wang, X.Y. Optimal operation of independent regional power grid with multiple wind-solar-hydro-battery power. *Appl. Energy* **2019**, *235*, 1541–1550. [[CrossRef](#)]
19. Li, H.H.; Mahmud, M.A.; Arzaghi, E.; Abbassi, R.; Chen, D.Y.; Xu, B.B. Assessments of economic benefits for hydro-wind power systems: Development of advanced model and quantitative method for reducing the power wastage. *J. Clean. Prod.* **2020**, *277*, 20. [[CrossRef](#)]
20. Jurasz, J.; Mikulik, J.; Krzywda, M.; Ciapala, B.; Janowski, M. Integrating a wind- and solar-powered hybrid to the power system by coupling it with a hydroelectric power station with pumping installation. *Energy* **2018**, *144*, 549–563. [[CrossRef](#)]
21. Duque, A.J.; Castronuovo, E.D.; Sanchez, I.; Usaola, J. Optimal operation of a pumped-storage hydro plant that compensates the imbalances of a wind power producer. *Electr. Power Syst. Res.* **2011**, *81*, 1767–1777. [[CrossRef](#)]
22. Li, F.F.; Qiu, J. Multi-objective optimization for integrated hydro-photovoltaic power system. *Appl. Energy* **2016**, *167*, 377–384. [[CrossRef](#)]
23. Liu, J.C.; Li, J.H.; Xiang, Y.; Hu, S. Optimal Sizing of Hydro-PV-Pumped Storage Integrated Generation System Considering Uncertainty of PV, Load and Price. *Energies* **2019**, *12*, 15. [[CrossRef](#)]
24. Dufo-Lopez, R.; Bernal-Agustin, J.L.; Contreras, J. Optimization of control strategies for stand-alone renewable energy systems with hydrogen storage. *Renew. Energy* **2007**, *32*, 1102–1126. [[CrossRef](#)]
25. Zhang, X.S.; Ma, G.W.; Huang, W.B.; Chen, S.J.; Zhang, S. Short-Term Optimal Operation of a Wind-PV-Hydro Complementary Installation: Yalong River, Sichuan Province, China. *Energies* **2018**, *11*, 868. [[CrossRef](#)]
26. Zhang, L.Q.; Xie, J.; Chen, X.Y.; Zhan, Y.S.; Zhou, L. Cooperative Game-Based Synergistic Gains Allocation Methods for Wind-Solar-Hydro Hybrid Generation System with Cascade Hydropower. *Energies* **2020**, *13*, 15. [[CrossRef](#)]
27. Xu, B.B.; Chen, D.Y.; Venkateshkumar, M.; Xiao, Y.; Yue, Y.; Xing, Y.Q.; Li, P.Q. Modeling a pumped storage hydropower integrated to a hybrid power system with solar-wind power and its stability analysis. *Appl. Energy* **2019**, *248*, 446–462. [[CrossRef](#)]
28. Tapia, A.; Tapia, G.; Ostolaza, J.X.; Saenz, J.R. Modeling and control of a wind turbine driven doubly fed induction generator. *IEEE. Trans. Energy Conver.* **2003**, *18*, 194–204. [[CrossRef](#)]

29. Guo, P. Variable pitch control of wind turbine generator combined with fuzzy feed forward and fuzzy PID controller. *Proc. Chin. Soc. Elect. Eng.* **2010**, *30*, 123–128. (In Chinese)
30. Guo, P. New variable pitch control strategy combining nonlinear feed forward and fuzzy PID control for wind turbine generator sets. *Chin. J. Power Eng.* **2010**, *30*, 838–843. (In Chinese)
31. Yang, J.X.; Zhu, L. Research on Photovoltaic Cell Model Based on MATLAB/Simulink. *Modern Electron. Tech.* **2011**, *34*, 24. (In Chinese)
32. Zhang, H.; Chen, D.Y.; Xu, B.B.; Wu, C.Z.; Wang, X.Y. The slow-fast dynamical behaviors of a hydro-turbine governing system under periodic excitations. *Nonlinear Dynam.* **2017**, *87*, 2519–2528. [[CrossRef](#)]
33. Wang, F.F.; Chen, D.Y.; Xu, B.B.; Zhang, H. Nonlinear dynamics of a novel fractional-order Francis hydro-turbine governing system with time delay. *Chaos Soliton. Fract.* **2016**, *91*, 329–338. [[CrossRef](#)]
34. Li, H.H.; Chen, D.Y.; Zhang, H.; Wang, F.F.; Ba, D.D. Nonlinear modeling and dynamic analysis of a hydro-turbine governing system in the process of sudden load increase transient. *Mech. Syst. Signal Process.* **2016**, *80*, 414–428. [[CrossRef](#)]

Publisher’s Note: MDPI stays neutral with regard to jurisdictional claims in published maps and institutional affiliations.



© 2020 by the authors. Licensee MDPI, Basel, Switzerland. This article is an open access article distributed under the terms and conditions of the Creative Commons Attribution (CC BY) license (<http://creativecommons.org/licenses/by/4.0/>).